Article No. mb982110 *J. Mol. Biol.* (1998) **283**, 657–668

JMB

Crystal Structures of Acutolysin A, a Three-disulfide Hemorrhagic Zinc Metalloproteinase from the Snake Venom of *Agkistrodon acutus*

Weimin Gong[1], Xueyong Zhu[1], Sijiu Liu[1], Maikun Teng[1] and Liwen Niu[1,2]*

[1]*Department of Molecular Biology and Cell Biology and Laboratory of Structural Biology, School of Life Science University of Science and Technology of China, CAS Hefei, Anhui 230026 P.R. China*

[2]*National Laboratory of Biomacromolecules, Institute of Biophysics, CAS, Beijing 100101, P.R. China*

**Corresponding author*

Acutolysin A alias AaHI, a 22 kDa hemorrhagic toxin isolated from the snake venom of *Agkistrodon acutus*, is a member of the adamalysin subfamily of the metzincin family and is a snake venom zinc metalloproteinase possessing only one catalytic domain. Acutolysin A was found to have a high-activity and a low-activity under weakly alkaline and acidic conditions, respectively. With the adamalysin II structure as the initial trial-and-error model, the crystal structures were solved to the final crystallographic *R*-factors of 0.168 and 0.171, against the diffraction data of crystals grown under pH 5.0 and pH 7.5 conditions to 1.9 Å and 1.95 Å resolution, respectively. One zinc ion, binding in the active-site, one structural calcium ion and some water molecules were localized in both of the structures. The catalytic zinc ion is coordinated in a tetrahedral manner with one catalytic water molecule anchoring to an intermediate glutamic acid residue (Glu143) and three imidazole $N^{\varepsilon 2}$ atoms of His142, His146 and His152 in the highly conserved sequence $H_{142}E_{143}XXH_{146}XXGXXH_{152}$. There are two new disulfide bridges (Cys157-Cys181 and Cys159-Cys164) in acutolysin A in addition to the highly conserved disulfide bridge Cys117-Cys197. The calcium ion occurs on the molecular surface. The superposition showed that there was no significant conformational changes between the two structures except for a few slight changes of some flexible residue side-chains on the molecular surface, terminal residues and the active-site cleft. The average contact distance between the catalytic water molecule and oxygen atoms of the Glu143 carboxylate group in the weakly alkaline structure was also found to be closer than that in the weakly acidic structure. By comparing the available structural information of the members of the adamalysin subfamily, it seems that, when lowering the pH value, the polarization capability of the Glu143 carboxylate group to the catalytic water molecule become weaker, which might be the structural reason why the snake venom metalloproteinases are inactive or have a low activity under acidic conditions.

Keywords: metalloproteinase; hemorrhagic toxin; snake-venom proteinase; metzincins; protein crystallography

Introduction

Metzincins can hydrolyze the internal peptide bonds of protein substrates at neutral or weakly alkaline pH values. Following astacin, a digestive metalloproteinase (Bode *et al*., 1992; Gomis-Rüth *et al*., 1994a), the structures of some other metzincins have also been determined such as adamalysin II (Gomis-Rüth *et al*., 1994b), atrolysin C (Zhang

Abbreviations used: SVMPs, snake-venom metalloproteinases; MMPs, matrix metalloproteinases; MIR, multiple isomorphous replacement.

E-mail address of the corresponding author: lwniu@ustc.edu.cn

0022–2836/98/430657–12 $30.00/0

et al., 1994), H_2-proteinase (Kumasaka *et al*., 1996), fibroblast collagenase (Lovejoy *et al*., 1994a,b; Borkakoti *et al*., 1994), neutrophil collagenase (Stams *et al*., 1994; Bode *et al*., 1994; Reinemer *et al*., 1994), serralysin (Baumann *et al*., 1993; Baumann, 1994), serratia proteinase (Hamada *et al*., 1996) and stromelysin-1 (Gooley *et al*., 1994). The metzincin family can be grouped into the four subfamilies of astacins, adamalysins (alias snake-venom metalloproteinases, SVMPs), matrixins (alias vertebrate collagenases or matrix metalloproteinases, MMPs) and serralysins (alias large bacteria zinc-endopeptidases), because these proteinases not only contain the virtually identical zinc-binding consensus sequence HEXXHXXGXXH and a highly conserved methionine-containing turn (Met-turn) but also topologically share the overall structural similarity, especially in the zinc-binding environment, for a hydrolysis reaction (Bode *et al*., 1993; Gomis-Rüth *et al*., 1994a,b; Hooper, 1994; Stöcker *et al*. 1995). Furthermore, the metzincins can be classified into the matrix metalloproteinase superfamily (MMP-superfamily) together with another large family of important zinc-endopeptidases including the bacterial zinc-endopeptidase thermolysin (Blundell, 1994; Holmes & Matthews, 1982), due to their similarities of both structural topology and zinc-binding environment. The structures of the members of the MMP-superfamily have been compared (Blundell, 1994) to understand their structure-function relationships, especially their involvements in various connective-tissue diseases such as arthritis and breast cancer and to supply possible and promising target models for related structure-based drug design.

More than one hundred SVMPs have been isolated and purified from various snake venoms. Some of these can also be named as snake-venom hemorrhagins or hemorrhagic toxins due to their ability to destroy the structures of capillary basement membranes and cause local hemorrhage after injection into experimental animals (Ownby, 1990). These SVMPs can be divided into four classes: P-I, P-II, P-III and P-IV according to the number of domains involved (Bjarnasson & Fox, 1995). In the larger SVMPs, the N-terminal catalytic domain is often followed by a disintegrin-like domain (P-II class) and sometimes in addition followed by a cysteine-rich domain (P-III class) and lectin domain (P-IV class). The P-I class, possessing only one N-terminal catalytic domain, can be further divided into two subclasses: P-IA with stronger hemorrhagic activity and P-IB with weaker or without hemorrhagic activity. In another point of view, the SVMPs and the mammalian reproductive tract proteins such as EAP I (Perry *et al*., 1992) and PH30 (Blobel *et al*., 1992) are together classified into a new family, reprolysins, due to the similarities in both sequence and domain organization (Bjarnason & Fox, 1995).

The crystal structures of three members of the adamalysins, adamalysin II (Gomis-Rüth *et al*., 1994b), atrolysin C (Zhang *et al*., 1994) and H_2-proteinase (Kumasaka *et al*., 1996) have been reported. They all belong to the P-IB subclass. The three-dimensional structural information of other classes needs to be further investigated. Adamalysin II was isolated from the western diamondback rattlesnake *Crotalus adamanteus*, atrolysin C from the eastern diamondback rattlesnake and H_2-proteinase from the Habu snake *Trimeresurus flavoviridis*. A zinc ion was found to be bound with four ligands: one water molecule and three imidazol $N^{\varepsilon 2}$ nitrogen atoms of histidine residues in the highly conserved characteristic sequence HEXXHXXGXXH. This water molecule is located in the neighborhood of the carboxylate group of the glutamate residue and is considered to be a base for nucleophilic attack on the carbonyl carbon atom of the sensitive peptide bond. However, the zinc ion is penta-coordinated in the active site of many other metzincins such as astacin. The fifth ligand in the astacin structure, the side-chain of a tyrosine residue, acts as the proton donor for the hydrolysis reaction (Gomis-Rüth *et al*., 1994a). Adamalysin II was crystallized under weakly acidic conditions (about pH 5.0) far from the optimal activity, and may be inactive; the fifth ligand, which should be the proton donor group for the proteolysis reaction in the structure, is still unknown. Moreover, the fifth ligand for zinc-ion binding was also not observed in the H_2-proteinase structure, although the enzyme was crystallized under weakly alkaline conditions (about pH 8.0) quite near the optimal activity.

There are plenty of hemorrhagic toxins in the snake venom of Chinese mainland *Agkistrodon acutus*, including the three small-size (22 kDa) AaHI, AaHII and AaHIII (Xu *et al*., 1981) and the medium-size (about 44 kDa) AaHIV (Zhu *et al*., 1997a). AaHI and AaHII can be classified into the P-IA subclass of SVMPs, and AaHIII into the P-IB subclass (Bjarnason & Fox, 1995). AaHIV was considered as a promising new member of the P-II class (Zhu *et al*., 1997a). AaHI possesses stronger hemorrhagic activity with the minimum hemorrhagic dose (MHD) of 0.4 g (Xu *et al*., 1981) and has a zinc ion and a calcium ion necessary to its proteolytic and hemorrhagic activities (Zhang *et al*., 1984). Its proteolytic activity was observed to be sensitive to pH values, in that the activity under weakly alkaline condition (pH 7.5) is about 100 times stronger than that under weakly acidic condition (pH 5.0; Zhu *et al*., 1997b). Previously, as a series of studies on the structure-function relationships of snake-venom hemorrhagic toxins, we have reported the crystallization and preliminary X-ray crystallographic analyses of AaHI (under pH 7.5 conditions; Gong *et al*., 1996a, 1997a), AaHIII (Gong *et al*., 1996b, 1997b) and AaHIV (Zhu *et al*., 1996). AaH I, II, III and IV will hereafter be referred to as acutolysin A, B, C and D, respectively, due to their metalloproteinase characteristics. Unfortunately, the whole amino acid sequences of these four proteinases have not been determined by chemical or cDNA sequencing. The better crys-

tals of acutolysin A have now been grown under weakly acidic (about pH 5.0) and weakly alkaline (about pH 7.5) conditions, and the crystals diffracted X-rays over 2.0 Å resolution (1 Å = 0.1 nm), which allowed us to recognize the possible amino acid sequence of acutolysin A by the electron densities at higher resolution. We have now finished the structural determination of acutolysin A crystallized under both conditions. The structural refinements were done with data over 2.0 Å resolution. The crystal structures of acutolysin C and D are being determined in our laboratory. Our purpose here is to give details about the crystallographic sequence and crystal structures of acutolysin A, and to discuss the possible structural implications for its biological functions.

Results and Discussion

Crystallographic sequence and overall structure

The current sequence of acutolysin A (Table 1) is about 50 to 85% homologous with some other SVMPs (hereafter the numbering refers to acutolysin A except in specified notes). Like any other members of this family, acutolysin A also has two highly conserved characteristic sequences $H_{142}E_{143}XXH_{146}XXGXH_{152}$ and $C_{164}I_{165}M_{166}$. Both acutolysin A and Ac1 are hemorrhagic proteinases; their sequences are very similar (85% homology for residues 1 to 200, 92% homology for residues 1 to 153 and 177 to 200) except for the segment of residues 154 to 176 (only 26% homology). In contrast, the sequence of residues 154 to 176 of acutolysin A is very homologous with that of ACLPREH (81% homology). Ac1 is a metalloproteinase isolated from the snake venom of the Chinese Taiwan *Agkistrodon acutus* (Nikai *et al.*, 1995). ACLPREH is also a metalloproteinase from the snake venom of the broad-banded copperhead *Agkistrodon contortrix laticinctus* (Selistre de Araujo & Ownby, 1995). Their N-terminal amino acid sequences are highly homologous with that of acutolysin A. The sequence of this segment in the acutolysin A structure has been validated repeatedly during the structural determination.

Table 1. Alignment of the current sequence of acutolysin A from *Agkistrodon acutus* with some of snake-venom metalloproteinases

	1 10 20 30 40 50
acutolysin A	STEFQRYMEIVIVVDHSMVKKYNGDSNSIKAWVYEMINTITESYSYLNID
Ac1	STEFQRYMEIVIVVDHSMVKKYNGDSPKIKAWVYEMINTITEGYRDLYID
ACLPREH	NYQYQRYVELVTVVDHGMYTKYNGDSDNIRQWVHQMVNTMKESYPYMYID
adamalysin II	<EQNLPQRYIELVVVADRRVFMKYNSDLNIIRTRVHEIVNIINEFYRSLNIR
atrolysin C	<EQNLPQRYIELVVVADHRVFMKYNSDLNTIRTRVHEIVNFINGFYRSLNIH
H_2-proteinase	ERFPQRYIELAIVVDHGMYKKYNQNSDKIKVRVHNMVNHINEMYRPLNIA

	51 60 70 80 90 100
acutolysin A	IILSGLEIWSEKDLINVEASAANTLKSFGEWRAKDLLHRISHDNAQLLTA
Ac1	IILSGLEIWSEKDLINVEASAGNTLKSFGEWRAKDLIHRISHDNAQLLTA
ACLPREH	ISLAGVEIWSNKDLIDVQPAARHTLDSFGEWRERDLLHRISHDNAQLLTS
adamalysin II	VSLTDLEIWSGQDFITIQSSSSNTLNSFGEWRERVLLTRKRHDNAQLLTA
atrolysin C	VSLTDLEIWSNEDQINIQSASSDTLNAFAEWRETDLLNRKRHDNAQLLTA
H_2-proteinase	ISLNRLNIWSKKDLITVKSASNVTLESFGNWRETVLLKQQNNDCAHLLTA

	101 110 120 130 140 150
acutolysin A	TDFDGATIGLAYTASMCNPKRSVGIIQDHSSVNRLVAITLAHEMAHNLGV
Ac1	TDFDGPTIGLAYVASMCEPKLSVGVIQDHSSVNRLVAITLAHEMAHNLGV
ACLPREH	TDFDGPTIGLAYVGTMCDPKLSTGVVEDHSKINFLVAVTMAHEMGHNLAM
adamalysin II	INFEGKIIGKAYTSSMCNPRSSVGIVKDHSPINLLVAVTMAHELGHNLGM
atrolysin C	IELDEETLGLAPLGTMCDPKLSIGIVQDHSPINLLMGVTMAHELGHNLGM
H_2-proteinase	TNLNDNTIGLAYKKGMCNPKLSVGLVQDYSPNVFMVAVTMTHELGHNLGM

	151 160 170 180 190 200
acutolysin A	SHDEGSCSCGGKSCIMSPSISDETSKYFSDCSYIQCRDYIAKENPPCILN
Ac1	RHDEKDCVGVVYLCIMRIPVVEDKRSYFSDCSYIQCREYISKENPPCILNKP
ACLPREH	RHDTGSCSCGGYSCIMSPVISDDSPKYFSNCSYIQCWDFIMKENPQCILNKP
adamalysin II	EHDGKDCLRGASLCIMRPGLTPGRSYEFSDDSMGYYQKFLNQYKPQCILNKP
atrolysin C	EHDGKDCLRGASLCIMRPGLTKGRSYEFSDDSMHYYERFLKQYKPQCILNKP
H_2-proteinase	EHDDKDKCKCEA-CIMSDVISDKPSKLFSDCSKNDYQTFLTKYNPQCILNA

<E denotes 5-pyrrolidone-2-carboxylic acid. The N-terminal 13 residues of acutolysin A were determined by the Edman degradation method and the others were defined crystallographically. Ac1 is a hemorrhagic proteinase from the Taiwan *Agkistrodon acutus* (Nikai *et al.*, 1995). The ACLPREH sequence is translated from a cDNA sequence of snake venom protein from the broad-banded copperhead *Agkistrodon contortrix laticinctus* (Selistre de Araujo & Ownby, 1995). Adamalysin II is a non-hemorrhagic proteinase from the Eastern diamondback rattlesnake *Crotalus atrox* and atrolysin C is a weaker hemorrhagic proteinase from the Western diamondback rattlesnake *Crotalus atrox* (Gomis-Rüth *et al.*, 1994b). H_2-proteinase is a non-hemorrhagic proteinase from *Trimeresurus flavoviridis* (Takeya *et al.*, 1989).

Acutolysin A has three disulfide connections: Cys117-Cys197, Cys159-Cys181 and Cys157-Cys164. All of the sequenced SVMPs have one conserved disulfide bridge: Cys117-Cys197. However, according to the number of variable disulfide bridges in the C-terminal subdomain and the local sequence environments around the disulfide bridges, it seems that these SVMPs could be recognized as four types as follows. (1) The residues 159 and 181 are both non-cysteine residues; they belong to the two-disulfide enzymes (Cys117-Cys197 and Cys157-Cys164) such as adamalysin II and atrolysin C. (2) Ac1 is the only one which has Cys181 and Gly159 instead of Cys159 and may also belong to the two-disulfide enzymes. (3) The residues 159 and 181 are both cysteine; they are among the three-disulfide enzymes (Cys117-Cys197, Cys159-Cys181 and Cys157-Cys164) such as acutolysin A. (4) The residues 159 and 181 are also both cysteine but there are some insertions and deletions around the cysteine residues such as in the H_2-proteinase sequence; they are also among the three-disulfide enzymes. Clearly, the whole amino acid sequence of acutolysin A should be determined by chemical and/or cDNA sequencing, which are being carried out in our department, to recognize the ambiguity between similar-sized residues, such as Gln and Glu, Asn and Asp, due to the relatively poor diffraction resolution limits of protein crystals.

There was no significant conformational changes between the two kinds of acutolysin A crystal structures except for a few flexible residue side-chains on the molecular surface and terminal residues. Therefore all the plots and descriptions of acutolysin A here were based on the weakly acidic structure except for those specially pointed out.

The overall structure of acutolysin A (Figure 1) is similar to those of adamalysin II and H_2-proteinase (Gomis-Rüth *et al.*, 1994b; Kumasaka *et al.*, 1996). It consists of two subdomains and has similar secondary structures to that of adamalysin II (about 40% α-helices and 20% β-strands). The major subdomain (alias upper subdomain, residues 4 to 152) exhibits the typical structural features of an α/β protein and has an open-sandwich topology, in which the α-helices are arranged on both sides of a twisted, five-stranded β-sheet; helices A, B and D are on one side and helix C on another side. The β-sheet is formed by four parallel strands, strands II, I, III and V, and an antiparallel strand, strand IV. The minor subdomain (alias lower subdomain, residues 153 to 200) consists of a long α-helix (helix E) and complicated loops. The three disulfide bridges and regular turns make the connections between the loops and stabilize their conformations.

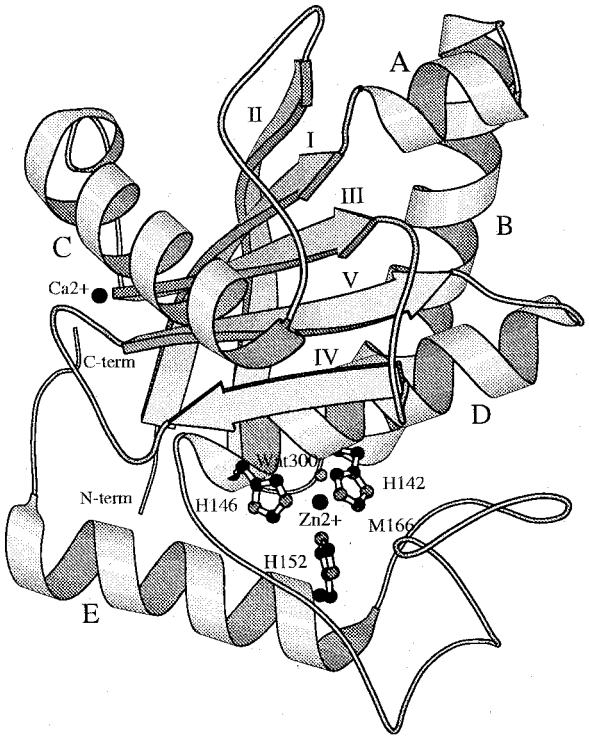

Figure 1. Overall structure of weakly acidic acutolysin A. The molecule is shown in standard orientation. The three disulfide connections, the calcium ion, the zinc ion (filled circles), and the three histidine zinc ligation residues are also shown. The Figure was produced using the program MOLSCRIPT (Kraulis, 1991).

The zinc-ion binding environment

Each member of the metzincins has a zinc ion in its active site. In the astacin structure, the zinc ion is penta-coordinated by the $N^{\varepsilon 2}$ nitrogen atoms of three histidine residues in the highly conserved sequence HEXXHXXGXXH, the side-chain of a tyrosine residue and one water molecule. In contrast, the tyrosine residue is replaced by proline or alanine residues in the adamalysins. The side-chain of Pro or Ala cannot be the chelators for zinc-ion binding. Therefore the manner of zinc-ion binding is tetrahedral in adamalysin II, atrolysin C and H_2-proteinase structures. As a member of the adamalysins, acutolysin A has a similar zinc-ion binding environment (Table 2 and Figure 2). The fourth ligand, water molecule 300, is close to the carboxylate group oxygen atoms of neighbor Glu143.

It was assumed that Glu143 could polarize water molecule 300 for the nucleophilic attack on the scissile peptide bond of a polypeptide chain substrate. The key role of water molecule 300 was confirmed by the structures of the complexes of atrolysin C with the inhibitors, in which the position of the fourth ligand was occupied by an oxygen atom of the inhibitor instead of the water molecule. The proteolytic activity of acutolysin A is as sensitive to lower pH as the other members of the metzincins. The optimal activity appears under neutral or weakly alkaline conditions. The contact distances of water molecule 300-Glu143 $O^{\delta 1}$ and water molecule 300-Glu143 $O^{\delta 2}$ in the weakly acidic structures are longer (4.19 Å and 3.85 Å, respectively)

Table 2. The bonds and angles in the active site of acutolysin A

Bonds (Å)			Angles (°)		
	pH 7.5	pH 5.0		pH 7.5	pH 5.0
His142 $N^{\varepsilon 2}$—Zn	2.07	2.05	His142 $N^{\varepsilon 2}$—Zn—His146 $N^{\varepsilon 2}$	94.38	99.86
His146 $N^{\varepsilon 2}$—Zn	2.10	2.26	His142 $N^{\varepsilon 2}$—Zn—His152 $N^{\varepsilon 2}$	104.89	106.28
His152 $N^{\varepsilon 2}$—Zn	2.09	2.27	His146 $N^{\varepsilon 2}$—Zn—His152 $N^{\varepsilon 2}$	107.02	96.75
Wat300—Zn	2.06	2.16	His142 $N^{\varepsilon 2}$—Zn—Wat300	105.47	114.52
Wat300—Glu143 $O^{\varepsilon 1}$	3.84	4.19	His146 $N^{\varepsilon 2}$—Zn—Wat300	110.04	111.91
Wat300—Glu143 $O^{\varepsilon 2}$	3.53	3.85	His152 $N^{\varepsilon 2}$—Zn—Wat300	129.29	123.71

Wat300 represents water molecule 300.

than that of good hydrogen bonding. Similar structural facts were also observed in other metzincins. Adamalysin II was crystallized around pH 5.0 and might be inactive. In the adamalysin II structure, the temperature factor of the catalytic water molecule is relatively high (31.62 $Å^2$) and the contact distance between the water molecule and Glu143 $O^{\delta 2}$ is too far (greater than 4.0 Å) for the formation of regular hydrogen bonding. However, in the structures of H_2-proteinase and our weakly alkaline acutolysin A which were crystallized, respectively, around pH 8.0 and pH 7.5 near the optimum pH for their proteolytic activity, the hydrogen-bonding distances between the catalytic water molecule and the Glu143 carboxylate group are shorter than those in adamalysin II and our weakly acidic acutolysin A structures (Table 3). The pK_a of the glutamate carboxylate group is around 4.3. When lowering the pH values, the polarization capabilities of the Glu143 carboxylate group to the catalytic water molecule become weaker and meanwhile the contact distance between the catalytic water molecule and the Glu143 carboxylate group becomes larger, which might be the structural reason why the metalloproteinases are inactive or have low activity under acidic conditions.

The proton donor should be present for the hydrolysis reaction of internal peptide bonds in protein substrates just as observed in the astacin structure. It is noteworthy that such a proton donor was not localized in adamalysin II, H_2-proteinase and our acutolysin A. These structural facts seem to lead to the following questions. Is the proton donor really supplied by the residue side-chains such as in the astacin structure? Are there other sources of proton donor in the process of the hydrolysis reaction? Does one of the structural binding water molecules in the active-site region lay this role? These questions have to be answered by further investigations in the future.

Configuration of the disulfide bonds

The metzincins have various numbers of disulfide bridges. A highly conserved disulfide bridge (Cys117-Cys197) connects two subdomains, while the variation of disulfide bridge numbers occurs in the C-terminal subdomain. Adamalysin II and atrolysin C have two disulfide bridges: Cys117-Cys197 and Cys157-Cys164. According to the amino acid sequences and fluorescence analysis (Takeya *et al.*, 1989), most of the SVMPs have two additional cysteine residues (Cys159 and Cys181) and should be three-disulfide enzymes. Acutolysin A has three disulfide bridges. The first disulfide bridge is again the highly conserved Cys117-

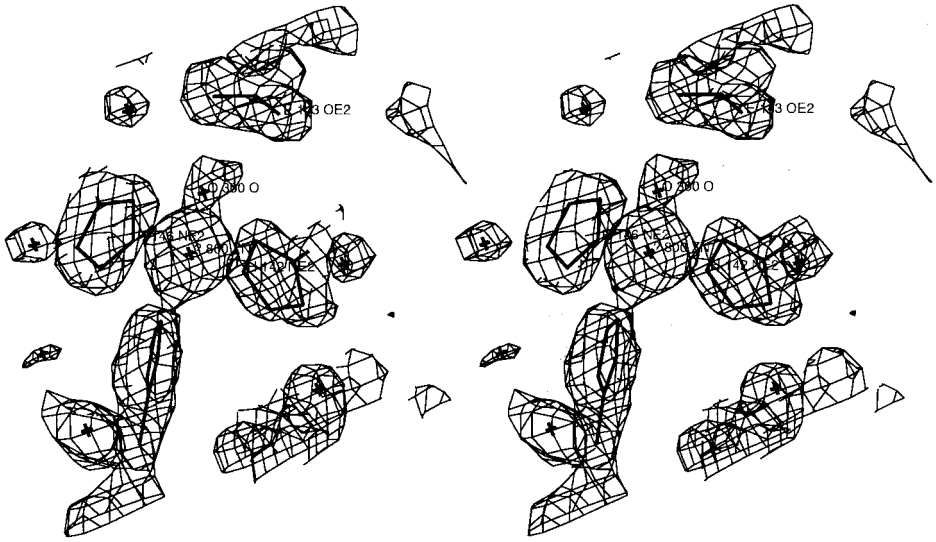

Figure 2. The active-site structure of acutolysin A superimposed with the electron densities. The plot was made using CHAIN (Sack, 1988).

Table 3. The contact distances between the catalytic water molecule and the Glu143 carboxylate group

	Acutolysin A	Adamalysin II	Acutolysin A	H2-proteinase
Crystallization pH value	5.0	5.0	7.5	8.0
Proteolytic activity	lower	lower	higher	higher
Wat300—$O^{\varepsilon 1}$ (Å)	4.19	4.11	3.84	–
Wat300—$O^{\varepsilon 2}$ (Å)	3.85	4.66	3.53	3.27

Adamalysin II data from Gomis-Rüth *et al.* (1994b); H_2-proteinase data from Kumasaka *et al.* (1996).

Cys197. Two additional connections are Cys157-Cys181 and Cys159-Cys164. These three disulfide bridges were observed clearly during the structural determination. By comparison between acutolysin A and H_2-proteinase, the disulfide bridges Cys117-Cys197 and Cys157-Cys181 have similar configuration in both structures, but the local environments around Cys159-Cys164 are very different (Figure 3) due to the difference of local insertion and deletion of amino acid residues.

Because of the formation of new disulfide bridges, the structures of residues 153 to 164 and 173 to 176 in acutolysin A are very different from those in adamalysin II, which should be the main reason why residues 154 to 176 can not be traced on the initial electron density maps after molecular replacement. Noticeably, the H_2-proteinase structure was solved independently by multiple isomorphous replacement (MIR); residues 155 to 175 had also not been traced with the initial MIR and solvent-flattening density maps (Kumasaka *et al.*, 1996). Such a structural segment containing many cysteine residues is not disordered and the electron densities should have a similar error level to other structural segments. Actually, after the completion of the adamalysin II structural determination, the possible conformational changes in three-disulfide enzymes had been predicted: the formation of both Cys157-Cys181 and Cys159-Cys164 would lead to larger movements of residues 153 to 160 and residue 176 (Gomis-Rüth *et al.*, 1994b). The structure of acutolysin A indeed confirmed such excellent prediction as well as H_2-proteinase. Since acutolysin A is hemorrhagic and H_2-proteinase non-hemorrhagic, it seems that the variable disulfide bridges in the C-terminal subdomain of the three-disulfide enzymes could not be considered as the direct factor of whether the proteinases have hemorrhagic activity or not.

Calcium-ion binding site

As with adamalysin II and atrolysin C, a calcium ion occurs on the surface of the acutolysin A molecule opposite to the active-site cleft and close to the crossover point of the N-terminal and the C-terminal segment. However, the calcium-binding characteristics were found to be slightly different under weakly acidic and alkaline conditions (Table 4). The calcium ion is liganded by seven and six oxygen atoms in weakly acidic and alkaline structures, respectively. The common calcium-ion

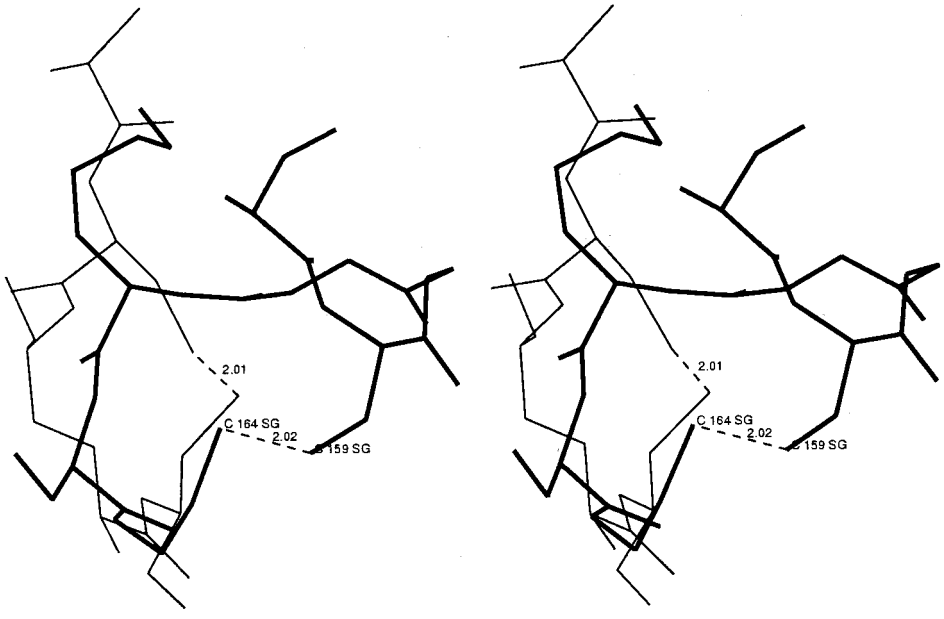

Figure 3. Superposition of the disulfide bridge Cys159-Cys164 of acutolysin A (thick line) and H_2-proteinase (thin line). The Sγ atoms of Cys159 and Cys164 of acutolysin A are labeled C 159 SG and C 164 SG, respectively. Disulfide bridges are indicated by broken lines and the figures against these broken lines are bond lengths (in Å).

Table 4. Bonds of the calcium-ion binding site (Å)

	pH 5.0	pH 7.5
Asn200 $O^{\delta1}$—Ca^{2+}	2.40	2.31
Cys197 O—Ca^{2+}	2.45	2.25
Asp93 $O^{\delta1}$—Ca^{2+}	2.52	2.38
Asp93 $O^{\delta2}$—Ca^{2+}	2.29	2.29
Glu9 $O^{\varepsilon1}$—Ca^{2+}	2.28	2.35
Water—Ca^{2+}	2.13	2.19
Water—Ca^{2+}	–	2.63

ligands are the carbonyl oxygen atom of Cys197, Asn200 $O^{\delta1}$, Glu9 $O^{\varepsilon1}$, Asp93 $O^{\delta1}$, Asp93 $O^{\delta2}$ and one water molecule. The seventh ligand in the weakly alkaline structure is also a water molecule. This might be a result of the fact that acutolysin A was crystallized in a different local microenvironment. Noticeably, no calcium ion could be found in the similar position of the H_2-proteinase structure, although this position has a very similar surrounding environment consisting of the conserved Cys197, Asn199, Glu9, Asp93 and a structural water molecule. Therefore, the manner of calcium binding might not directly affect the enzymatic activities since this site is far from the active site; no significant conformational change could be caused by the differences of calcium-ion binding. It has been pointed out (Gomis-Rüth *et al.*, 1994b) that the importance of the calcium ion might be for the structural integrity of the proteolytic domain. Due to its position close to the C terminus, this calcium ion in the multidomain parent structure could well play an important role in stabilizing and tightening the segment connecting the proteolytic domain with the succeeding disintegrin domain. We are determining the crystal and molecular structure of acutolysin D, a medium-size P-II-type snake-venom metalloproteinase mentioned above, and waiting for the structural details of the connecting region between the proteolytic and disintegrin domains.

Implications for the hemorrhagic activity

Acutolysin A has a strong hemorrhagic activity. In contrast, adamalysin II and H_2-proteinase are both non-hemorrhagic, and atrolysin C has a weak hemorrhagic activity. The sequence alignment of all snake-venom metalloproteinases showed that no residue substitution is key and necessary to their hemorrhagic activities. Therefore, the question of why some of the metalloproteinases are hemorrhagic and others are not must be answered according to their three-dimensional structures rather than their primary sequences. The enzymolysis sites of both acutolysin A and adamalysin II for insulin B-chain substrate are almost same (Xu *et al.*, 1995), which means that the different hemorrhagic activities of these two proteinases might not directly be due to their hydrolysis specificity. Acutolysin A and adamalysin II might possess different capabilities in binding with the proteins in the basement membranes of blood capillaries. The overall structures of acutolysin A, H_2-proteinase and adamalysin II are very similar except for two segments: residues 153 to 164 and residues 173 to 176 (Figure 4) due to the different disulfide connections. The segment of residues 164 to 172 are structurally similar. The residues Cys164 to Ser167 construct the characteristic active-site basement: Met-turn. The main-chains of Pro168-Ser169-Ile170 are the part of the active-site pocket. These structural features show that acutolysin A and adamalysin II have similar active pockets for proteolytic reaction. The difference of hemorrhagic activity must be revealed in the crystal structures. However, it seems that the structural difference of residues 153 to 176 was not certainly related to hemorrhagic activity. This small amount of struc-

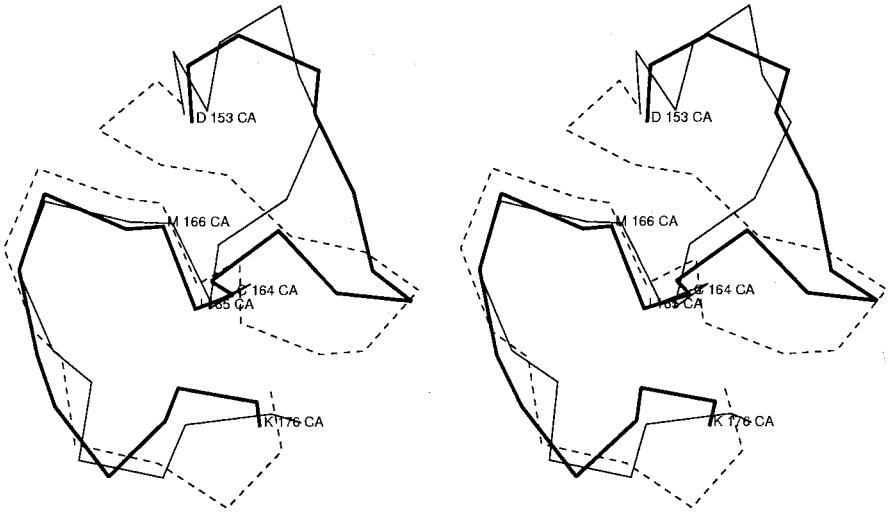

Figure 4. Superposition of C^{α} structures of residues 153 to 176 of acutolysin A (thick line), adamalysin II (broken line), and H_2-proteinase (thin line). The residues Asp153, Cys164, Ile165, Met166 and Lys176 are labeled. The plot was made using CHAIN (Sack, 1988).

tural perturbation might be caused only by the insertion of the additional disulfide connection (Kumasaka *et al*., 1996; Jia *et al*., 1996). It has been observed (Xu *et al*., 1995) that acutolysin A marked by ^{125}I could be combined with nothing but the capillary blood vessel. We infer that capillary blood vessels perhaps have a special combination site for hemorrhagic snake-venom metalloproteinases, and that hemorrhagic snake-venom metalloproteinases possess the related recognition site, which might be one of the reasons that some snake-venom metalloproteinases are hemorrhagic and others are not. We cannot identify which residues and/or which local regions on the molecular surface of acutolusin A are the key sites to the hemorrhagic activity because we have only the crystallographic sequence instead of the real chemical sequence. As a whole, the real reason is still not very clear, and all sorts of hypotheses of hemorrhagic mechanism should be considered as possibilities which remain to be proved.

Comparison of weakly acidic and alkaline acutolysin A structures

As mentioned above, the overall structures of acutolysin A under different pH values have no significant changes. However, a small amount of conformational difference was found in the active site in terms of the contact distances between the zinc ion and the four ligands, three histidine groups and one catalytic water molecule, and between the water molecule and the side-chain of the catalytic glutamate residue, Glu143. The molecular superposition around the zinc ion environment (Figure 5) showed that the contact distances of the two imidazole $N^{\varepsilon 2}$ atoms of His146 and His152 to the catalytic zinc ion are shorter under pH 7.5 conditions than those under pH 5.0. The average contact distance between the catalytic water molecule and the oxygen atoms of the carboxylate group of Glu143 in the weakly alkaline structure was also found to be shorter than that in the weakly acidic structure. This phenomenon could be called a contraction. We do not know whether this small change in the active-site is related to the enzymatic function (such as proteolytic action) or not. As a possibility that should be checked out, the slight change in the active site under different pH values might result from errors during the structural determination. It is still unclear to us whether this contraction phenomenon is general or not. It should be pointed out that the slight conformational change in the active site is considered only as a phenomenon based on the comparison of two acutolysin A structures, and there is no other evidence of such as structural comparisons of homologous proteins with themselves at different proteolytic activity to prove this proposal.

Materials and Methods

Preparation and crystallization

The procedures for the purification of acutolysin A (Xu *et al*., 1981) were mainly modified as follows. The

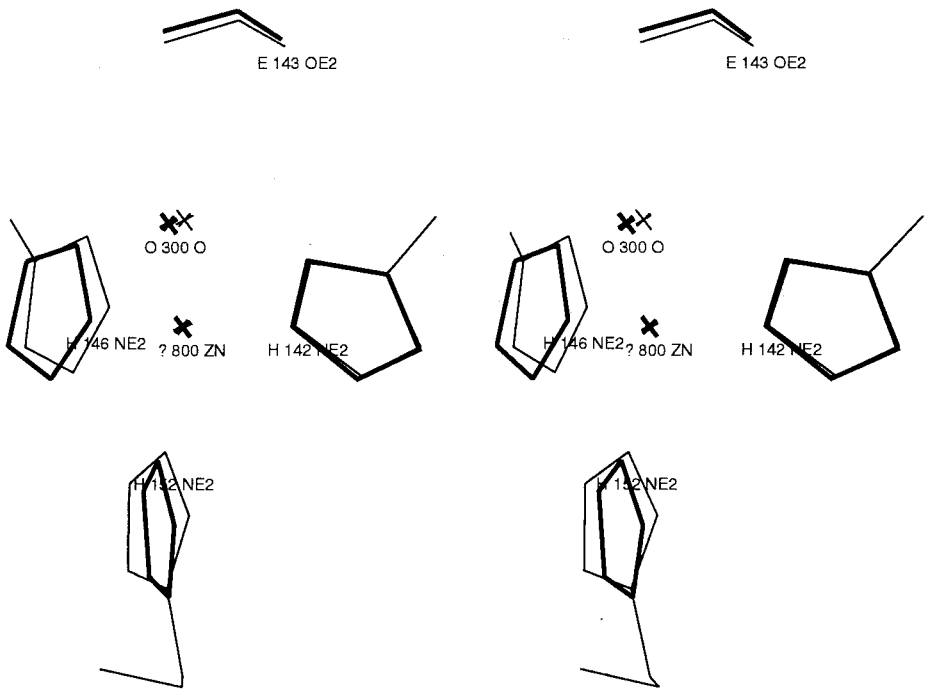

Figure 5. Superposition of the active-sites of weakly acidic acutolysin A (thick line) and weakly alkaline acutolysin A (thin line). The catalytic zinc ions are overlapped. Only the liganding atoms and Glu143 $O^{\varepsilon 1}$ are labeled. The plot was made using CHAIN (Sack, 1988).

venom powder was dissolved in 0.02 M Tris-HCl buffer (pH 8.0). The venom solution was applied to a DEAE-Sepharose Fast Flow S-200 (Pharmacia) column which had been equilibrated with the same buffer, and then eluted with a linear gradient from 0.02 M Tris-HCl buffer (pH 8.0) to 0.02 M Tris-HCl buffer (pH 6.0), containing 0.5 M NaCl. The fraction containing acutolysin A was collected, dialyzed against distilled water, concentrated and further purified by gel filtration on a S-200 Sephacryl (Pharmacia) column equilibrated and eluted with NaCl solution (0.15 M). All the purification steps were done at room temperature (about 25°C). Approximately 20 mg of purified acutolysin A was obtained from 1 g of crude venom.

The crystallization under weakly alkaline (pH 7.5) conditions and preliminary X-ray crystallographic analysis have been reported (Gong *et al*., 1996a,b). The better crystals with higher resolution were grown using similar procedures and slightly improved conditions. By the hanging-drop vapor diffusion method (McPherson, 1982) at room temperature, 4 μl of the precipitating solution containing 51% (v/v) MPD was mixed with 4 μl of the 20 mg/ml acutolysin A solution and then equilibrated against 0.5 ml of precipitating solution. These solutions were buffered with 0.02 M Tris-HCl (pH 7.5) and 0.02 M NaAc-HAc (pH 5.0), respectively. The tetragonal bipyramid-shaped crystals appeared under both conditions one week later.

Table 5. Data collection and refinements of acutolysin A structures

Crystallization pH	5.0	7.5
Space group	$P4_32_12$	$P4_32_12$
Cell dimensions		
a (Å)	63.47	63.17
c (Å)	95.49	94.35
Resolution ranges (Å)	8.0 to 1.9	10.0 to 1.95
Independent reflections[a]	11,789	12,809
Completeness (%)[b]	88.0	88.3
Last shell completeness (%)	74.5	76.6
R_{merge}[c]	5.0	8.3
Number of water molecules	233	152
Number of metal ions	2	2
R-factor[e]	0.168	0.171
Bond length r.m.s. deviation (Å)[e]	0.013	0.013
Bond angle r.m.s. deviation (°)[e]	1.34	1.60
Average temperature factors (Å^2):		
All atoms	17.54	17.85
Protein atoms	14.76	15.94
Main-chain atoms	13.41	14.66
Side-chain atoms	16.21	17.31
Water molecules	35.86	38.36

[a] The reflections are the ones of $F_{obs} > 1.0\sigma$ (F_{obs}).
[b] Completeness is the ratio of the number of observations to that of possible reflections.
[c] $R_{merge} = \Sigma_h\Sigma_i|I(h)_i - \langle I(h)\rangle|/\Sigma_h\Sigma_i I(h)_i$.
[d] $R\text{-factor} = \Sigma_h|F(h)_{calc} - F(h)_{obs}|/\Sigma_h F(h)_{obs}$.
[e] The ideal stereochemical parameters are the ones derived from the Cambridge database (Engh & Huber, 1991).

Data collection and reduction

At room temperature, the data of weakly acidic acutolysin A were collected from one crystal on a Siemens X200B multiwire area detector mounted on a Rigaku rotating anode X-ray generator at the National Laboratory of Biomacromolecules, Beijing. The nickel-filtered CuKα X-rays were generated at 50 kV and 200 mA without a double mirror system. The frame data were indexed, integrated, scaled and reduced using the XENGEN package (Howard *et al*., 1987).

For weakly alkaline acutolysin A, the data collection was completed at room temperature from one crystal by a MarResearch Imaging Plate (diameter 300 mm) mounted on a MarResearch sealed copper-target tube X-ray generator with graphite monochromator at our laboratory. The working tube voltage and current were 40 kV and 50 mA. The data were processed and scaled with DENZO and SCALEPACK, respectively (Otwinowski, 1993; Minor, 1993).

The preliminary X-ray crystallographic analysis showed that both crystals of acutolysin A belong to space group $P4_32_12$ or $P4_12_12$. According to the molecular mass and cell dimensions, one enzyme molecule is present in the asymmetric unit. Data collection and reduction statistics are summarized in Table 5.

Structural determination and refinement

With the adamalysin II structure as the initial trial-and-error model, the phasing of the acutolysin A weakly acidic crystal was performed by molecular replacement using the X-PLOR package (Brünger, 1992). In phasing the weakly acidic crystal structure by molecular replacement, some of the protein atoms in the adamalysin II structure were removed, including the side-chains of 76 residues which are highly variable in most of the SVMPs, the first three N-terminal residues and the last two C-terminal residues; all of the metal ions and solvent molecules were also deleted; the temperature factors of all atoms were set to an overall value of 15 Å^2. The correct space group of acutolysin A crystals was recognized as $P4_32_12$ mainly by the results of molecular replacement and confirmed by the sequential structural refinements. The model after translation was refined by ten cycles of rigid-body refinement against the data up to 3.0 Å resolution.

With the model given by molecular replacement and the data up to 1.9 Å resolution, the initial crystallographic *R*-factor was 0.40 and the initial electron density map showed that the model fitted the densities well except the main-chains and side-chains of residues 154 to 176 and part of the side-chains of other residues. All of the side-chains of these ''bad residues'' were deleted from the model and all of the main-chains of residues 154 to 176 were maintained but their crystallographic occupancy factors were assigned to be zero in order to cancel their contributions to the structural factors. Dramatically, several cycles of X-PLOR SA refinement gave a lower *R*-factor of 0.26. The *R*-factor dropped to 0.23 after several further cycles of conventional restrained positional refinements. Two relatively heavy density peaks representing the metal ions (one Zn^{2+} and one Ca^{2+}) at the positions similar to those in the adamalysin II structure and the densities of most of the main and side-chains were clear and easily recognized. Based on the homologous amino acid sequences, especially those of Ac1 and ACLPREH, and considering the local sizes and chemical environment of electron densities, the structures of the main-chains of residues 154 to 176 and all of side-chains were rebuilt by hand with computer graphics. Several further cycles of restrained positional refinement brought the *R*-factor to 0.22. Then the water molecules were added to the residual peaks on $2F_o - F_c$ or $F_o - F_c$ maps to match the stereochemical conditions. At this stage, all the residues and water molecules were

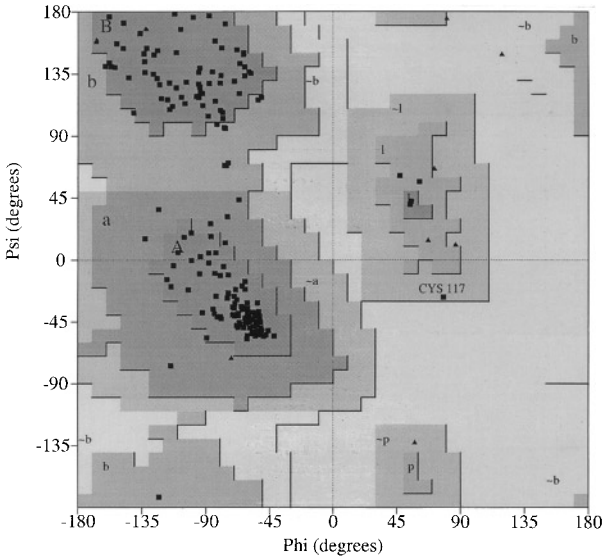

Figure 6. Ramachandran plot of acutolysin A. The main-chain conformational angles (Phi and Psi) of all non-glycine residues (indicated by a box), except Cys117, lie within the allowed low-energy regions (indicated by continuous boundaries). Glycine residues are indicated by a triangle. The plot was made using PROCHECK (CCP4, 1994).

checked once again and all the possible errors in the model corrected on the improved electron density maps. Then all the atomic positions and individual temperature factors were refined alternatively.

With the refined acutolysin A weakly acidic structure as an initial model, the weakly alkaline structure was refined with the data up to 1.95 Å resolution. The refinement results are listed in Table 5. Nine residues in the crystallographic sequence of the weakly acidic model were found to be wrong and adjusted again according to the weakly alkaline structure. Then all the atomic positions and individual temperature factors were refined and cross-validated once again. The refinement results of the weakly acidic structure are also listed in Table 5.

All of the main-chain conformational angles in both acutolysin A structures, except the Cys117 residues, are of low energy (Figure 6; Ramakrishnan & Ramachandran, 1965). However, the uncommon conformational angles of the Cys117 residues in the structures were clearly defined by the electron densities and also observed in the adamalysin II and H_2-proteinase structures, which might be a result of the highly conserved disulfide bridge Cys117-Cys197 in adamalysins.

The model rebuilding on the electron density maps was performed using the computer graphics program package CHAIN (Sack, 1988). The N-terminal 13 residues were sequenced by the Edman degradation method (Gong *et al*., 1996c) when the structural refinements were being done. No density was found for the N-terminal three residues (Ser1, Thr2 and Glu3) and two residues (Ser1 and Thr2) in the weakly acidic and alkaline structures, respectively, which might be disordered and undefined crystallographically. The peptide chain electron densities were found to end at Asn200, although the other small-size SVMPs often have residues 201 and 202. We do not know whether these two residues are absent or disordered crystallographically because the C-terminal sequence of acutolysin A has not been determined by chemical sequencing.

The coordinates of the acutolysin A structures were deposited with the Brookhaven Protein Data Bank (PDB codes: 1BSW and 1BUD) and are available on request.

Acknowledgments

The kind supply of the structural coordinates of adamalysin II by Dr Wolfram Bode of the Max-Planck-Institut fur Biochemie, Germany, atrolysin C by Dr Edgar Meyer of the Texas A and M University, USA, and H_2-proteinase by Dr Takashi Kusamaka of the Institute of Physical and Chemical Research (RIKEN), Japan, are gratefully acknowledged. Finanical support for this project to L.N. was provided by research grants from the Chinese Academy of Sciences, National Laboratory of Biomacromolecules and State Education Commission of China.

References

Baumann, U. (1994). Crystal structure of the 50 kDa metalloprotease from *Serratia marcescens*. *J. Mol. Biol.* **242**, 244–251.

Baumann, U., Wu, S., Flaherty, K. M. & McKay, D. B. (1993). Three-dimensional structure of the alkaline protease of *Pseudomonas aeruginosa*: a two-domain protein with a calcium binding parallel beta roll motif. *EMBO J.* **12**, 3357–3364.

Bjarnason, J. B. & Fox, J. W. (1995). Snake venom metallo-proteinases: reprolysins. *Methods in Enzymol.* **248**, 345–368.

Blobel, C. P., Wolfsberg, T. G., Turck, C. W., Myles, D. G., Primakoff, P. & White, J. M. (1992). A potential fusion peptide and an integrin ligand domain in a protein active in sperm-egg fusion. *Nature,* **356**, 248–252.

Blundell, T. L. (1994). Metalloproteinase superfamilies and drug design. *Nature Struct. Biol.* **1**, 73–75.

Bode, W., Gomis-Rüth, F. X., Huber, R., Zwilling, R. & St(cker, W. (1992). Structure of astacin and implications for activation of astacins and zinc-ligation of collagenases. *Nature,* **358**, 164–167.

Bode, W., Gomis-Rüth, F. X. & Stücker, W. (1993). Astacins, serralysins, snake venom and matrix metalloproteinase exhibit identical zinc-binding environments (HEXXHXXGXXH and Met-turn) and topologies and should be grouped into a common family, the 'metzincins'. *FEBS Letters,* **331**, 134–140.

Bode, W., Reinemer, P., Huber, R., Kleine, T., Schnierer, S. & Tschesche, H. (1994). The crystal structure of human neutrophil collagenase inhibited by a substrate analog reveals the essentials for catalysis and specificity. *EMBO J.* **13**, 1263–1269.

Borkakoti, N., Winkler, F. K., Williams, D. H., D'Arcy, A., Broadhurst, M. J., Brown, P. A., Johnson, W. H. & Murray, E. J. (1994). Structure of the catalytic domain of human fibroblast collagenase complexed with an inhibitor. *Nature Struct. Biol.* **1**, 106–110.

Brünger, A. T. (1992). *X-PLOR Version 3. 1. A System for X-ray Crystallography and NMR*, Yale University Press, New Haven and London.

CCP4 (1994). The CCP4 suite: programs for protein crystallography. *Acta Crystallog. sect. D,* **50**, 760–763.

Engh, R. A. & Huber, R. (1991). Accurate bond and angle parameters for X-ray protein structure refinement. *Acta Crystallog. sect. A,* **47**, 392–400.

Gomis-Rüth, F. X., Stöcker, W., Huber, R., Zwilling, R. & Bode, W. (1994a). Refined 1.8 Å X-ray crystal structure of astacin, a zinc-endopeptidase from the crayfish *Astacus astacus* L. *J. Mol. Biol.* **229**, 945–968.

Gomis-Rüth, F. X., Kress, L. F., Kellermann, J., Mayr, I., Lee, X., Huber, R. & Bode, W. (1994b). Refined 2.0 Å X-ray crystal structure of the snake venom zinc-endopeptidase adamalysin II: primary and tertiary structure determination, refinement, molecular structure and comparison with astacin, collagenase and thermolysin. *J. Mol. Biol.* **239**, 513–544.

Gong, W., Zhu, Z., Niu, L. & Teng, M. (1996a). Crystallization and preliminary X-ray diffraction studies of Hemorrhagin I from the snake venom of *Agkistrodon acutus*. *Acta Crystallog. sect. D,* **52**, 201–202.

Gong, W., Zhu, Z., Niu, L. & Teng, M. (1996b). Preliminary X-ray diffraction analysis of haemorrhagin III from the snake venom of *Agkistrodon acutus*. *Chinese Sci. Bulletin.* **42 (4)**, 544–546.

Gong, W., Zhu, Z., Niu, L., Teng, M., Wang, C. & Shen, W. (1996c). Preliminary amino acid sequences analysis of haemorrhagin I from the snake venom of *Agkistrodon acutus*. *J. Univ. Sci. Tech. China.* **26(9)**, 366–368.

Gong, W., Teng, M. & Niu, L. (1997a). 0.27 nm resolution crystal structure of haemorrhagin I from the snake venom of *Agkistrodon acutus*. *Chinese Sci. Bulletin.* **42(4)**, 333–337.

Gong, W., Teng, M. & Niu, L. (1997b). Crystal structure determination of alkaline haemorrhagin AaH-III from the snake venom of *Agkistrodon acutus*. *Sci. China (ser. C),* **40(4)**, 351–355.

Gooley, P. R., O'Connell, J. F., Marcy, A. I., Cuca, G. C., Salowe, S. P., Bush, B. L., Hermes, J. D., Esser, C. K., Hagmann, W. K., Spinger, J. P. & Johnson, B. A. (1994). The NMR structure of the inhibited catalytic domain of human stromelysin-1. *Nature Struct. Biol.* **1**, 111–118.

Hamada, K., Hata, Y., Katsuya, Y., Hiramatsu, H., Fujiwara, T. & Katsube, Y. (1996). Crystal structure of *serratia* proteinase, a zinc-depedent proteinase from *serratia* sp. E-15, containing a β-sheet coil motif at 2.0 Å resolution. *J. Biochem.* **119**, 844–851.

Holmes, M. A. & Matthews, B. W. (1982). Structure of thermolysin refined at 1.6 Å resolution. *J. Mol. Biol.* **160**, 623–639.

Hooper, N. M. (1994). Families of zinc-metalloproteinases. *FEBS Letters,* **354**, 1–6.

Howard, A. J., Gilliland, G. L., Finzel, B. C., Poulos, T. L., Ohlendorf, D. H. & Salemme, F. R. (1987). The use of an imaging proportional counter in macromolecular crystallography. *J. Appl. Crystallog.* **20**, 383–387.

Jia, L. G., Shimokawa, K. I., Bjarnason, J. B. & Fox, J. W. (1996). Snake venom metalloproteinases: structure, function and relationship to the adams family of proteins. *Toxicon,* **34**, 1269–1276.

Kraulis, P. J. (1991). MOLSCRIPT: a program to produce both detailed and schematic plots of protein structures. *J. Appl. Crystallog.* **24**, 946–950.

Kumasaka, T., Yamamoto, M., Moriyama, H., Tanaka, N., Sato, M., Katsube, Y., Yamakawa, Y., Omori-Satoh, T., Iwanaga, S. & Ueki, T. (1996). Crystal structure of H_2-proteinase from the venom of *Trimeresurus flavoviridis*. *J. Biochem.* **119**, 49–57.

Lovejoy, B., Cleasby, A., Hassell, A. M., Longley, K., Luther, M. A., Weigl, D., McGeahan, G., McElroy, A. B., Drewry, D., Lambert, M. H. & Jordan, S. R. (1994a). Structures of the catalytic domain of fibroblast collagenase complexed with an inhibitor. *Science,* **263**, 375–377.

Lovejoy, B., Hassell, A. M., Luther, M. A., Weigl, D. & Jordan, S. R. (1994b). Crystal structures of recombinant 19-kDa human fibroblast collagenase complexed to itself. *Biochemistry,* **33**, 8207–8217.

McPherson, A. (1982). *Preparation and Analysis of Protein Crystals*, John Wiley & Sons, New York.

Minor, W. (1993). *XDISPLAYF Program*, Purdue University.

Nikai, T., Kato, C., Komori, Y., Nodani, H., Homma, M. & Sugihara, H. (1995). Primary structure of Ac1-proteinase from the venom of *Deinagkistrodon acutus*. (Hundred-pace snake) from Taiwan. *Biol. Pharm. Bulletin,* **18(4)**, 631–633.

Otwinowski, Z. (1993). Oscillation data reduction program. In *Proceedings of the CCP4 Study Weekend: Data Collection and Processing*, 29–30, (compiled by Sawyer, L., Isaacs, N. & Bailey, S.), pp. 56–62, SERC Daresbury, UK.

Ownby, C. L. (1990). Locally acting agents: myotoxins, hemorrhagic toxins and dermonecrotic factors. In *Handbook of Toxinology* (Shier, W. T. & Mebs, D., eds), pp. 601–654, Marcel Dekker, Inc., New York.

Perry, A. C. F., Jones, R., Barker, P. J. & Hall, L. (1992). A mammalian epididymal protein with remarkable sequence similarity to snake venom haemorrhagic peptides. *Biochem. J.* **286**, 671–674.

Ramakrishnan, C. & Ramachandran, G. N. (1965). Stereochemical criteria for polypeptide and protein chain comformations II. Allowed conformations for a pair of peptide units. *Biophys. J.* **5**, 909–933.

Reinemer, P., Grams, F., Huber, R., Kleine, T., Schnierer, S., Pieper, M., Tschesche, H. & Bode, W. (1994). Structural implications for the role of the N-terminus in the superactivation of collagenases. A crystallographic study. *FEBS Letters,* **338**, 227–233.

Sack, J. S. (1988). CHAIN – a crystallographic modeling program. *J. Mol. Graphics.* **6**, 224–225.

Selistre de Araujo, H. S. & Ownby, C. L. (1995). Molecular cloning and sequence analysis of cDNA for metalloproteinases from broad-banded copperhead *Agkistrodon contortrix laticinctus*. *Arch. Biochem. Biophys.* **320**, 141–148.

Stams, T., Spurlino, J. C., Smith, D. L., Wahl, R. C., Ho, T. F., Qoronfleh, M. W., Banks, T. M. & Rubin, B. (1994). Structure of human neutrophil collagenase reveals large S1′ specificity pocket. *Nature Struct. Biol.* **1**, 119–123.

Stöcker, W., Grams, F., Baumann, U., Reinemer, P., Gomis-Rüth, F. X., McKay, D. B. & Bode, W. (1995). The metzincins: topological and sequential relations between the astacins, adamalysins, serralysins, and matrixins (collagenases) define a superfamily of zinc-peptidases. *Protein Sci.* **4**, 823–840.

Takeya, H., Arakawa, M., Miyata, T., Iwanaga, S. & Omori-Satoh, T. (1989). Primary structure of H_2-proteinase, a non hemorrhagic metalloproteinase isolated from the venom of the habu snake *Trimeresurus flavorviridis*. *J. Biochem.* **106**, 151–157.

Xu, X., Wang, C., Liu, J. & Lu, Z. (1981). Purification and characterization of hemorrhagic components

from *Agkistrodon acutus* (hundred pace snake) venom. *Toxicon,* **19**, 633–644.

Xu, X., Wang, Y., Wei, C. & Zhu, X. (1995). Study on the action mechanism of hemorrhagin I from *Agkistrodon acutus* venom. *Natural Toxin II,* 361–366.

Zhang, D., Botos, I., Gomis-Rüth, F. X., Doll, R., Blood, C., Njoroge, F. G., Fox, J. W., Bode, W. & Meyer, E. (1994). Structure interaction of natural and synthetic inhibitors with the venom metalloproteinase, atrolysin C (form-d). *Proc. Natl. Acad. Sci. USA,* **91**, 8447–8451.

Zhang, J., Chen, Z., He, Y. & Xu, X. (1984). Effect of calcium on proteolytic activity and conformation of hemorrhagic toxin I from five pace snake (*Agkistrodon acutus*) venom. *Toxicon,* **22**, 931–935.

Zhu, Z., Gong, W., Niu, L., Teng, M. & He, H. (1996). Purification, crystallization and preliminary X-ray diffraction analysis of haemorrhagin IV from the snake venom of *Agkistrodon acutus*. *Acta Crystallog. sect. D,* **52**, 407–408.

Zhu, Z., Gong, W., Zhu, X., Teng, M. & Niu, L. (1997a). Purification, characterization and conformation of a haemorrhagin from the venom of *Agkistrodon acutus*. *Toxicon,* **35**, 283–292.

Zhu, X., Zhu, Z., Gong, W., Teng, M. & Niu, L. (1997b). Studies on the relationship between the biological activities and the circular dichroism of south Anhui *Dienagkistrodon acutus* hemorrhagins. *Biochim. Biophys. Acta Sinica,* **29 (2)**, 53–29.

Edited by R. Huber

(Received 22 September 1997; received in revised form 27 July 1998; accepted 3 August 1998)